Implementation and features of nodal points in phonon spectra of crystals of the A15 family

Ivan Nebola
Uzhhorod National University
Uzhhorod, Ukraine
ivan.nebola@uzhnu.edu.ua

Diana Kaynts
Uzhhorod National University
Uzhhorod, Ukraine
diana.kaynts@uzhnu.edu.ua

Andrii Korneichuk
Uzhhorod National University
Uzhhorod, Ukraine
andrii.korneichuk@uzhnu.edu.ua

Mykola Pino
Uzhhorod National University
Uzhhorod, Ukraine
mykola.pino@uzhnu.edu.ua

Zosimov Rostyslav
Uzhhorod National University
Uzhhorod, Ukraine
rostyslav.zosimow@uzhnu.edu.ua

INTRODUCTION

The constraints arising from group-theoretical analysis had long been regarded in condensed matter physics as fundamental and practically indisputable; therefore, the emergence of works predicting stable fourfold and sixfold degeneracies became one of the most remarkable developments in the modern theory of phonon spectra [1–3]. In Ref. [3], a classification of all possible multiple phonon nodes — twofold, threefold, fourfold, and sixfold — was carried out on the basis of irreducible representations of little space groups. It was shown that sixfold nodal points may occur in crystals with space groups No. 218, 220, 222, 223, and 230, including materials such as C_3N_4, Sc_4C_3, Y_4Sb_3, and K_8Si_{46}.In recent years, our research interest has been focused on calculations of model phonon spectra and phonon densities of states for A15-family crystals described by space group 223. Particular attention has been attracted by robust sixfold degeneracies at the R point of the Brillouin zone revealed in the calculated model spectra of V3Si and Nb3Si. The obtained results were found to be stable with respect to variations of the model parameters and may be considered as a characteristic feature of lattice dynamics in A15-type crystals.Of particular interest is the comparison of phonon spectra and phonon densities of states for V3Si and Nb3Si, which, despite possessing the same structural type, exhibit noticeably different superconducting characteristics. V3Si is known for its relatively high superconducting transition temperature and pronounced electron-phonon interaction effects, whereas Nb3Si demonstrates a different character of lattice dynamics that may be reflected in the structure of phonon modes and densities of states. In the present work, model phonon spectra and phonon densities of states for these compounds are presented and the features of realization of multiply degenerate nodal points in A15-family crystals are discussed.

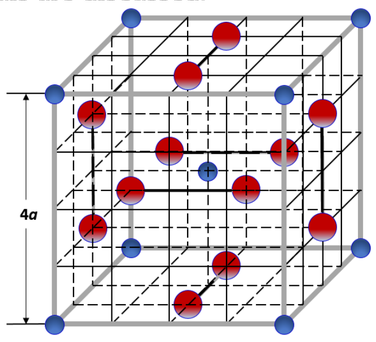

Fig. 1. Elementary cell of the A15 family represented as a (4a×4a×4a)(4a \times 4a \times 4a)(4a×4a×4a) superlattice based on a simple cubic lattice (SCL) with lattice parameter (ахала).

CONCLUSIONS

The presented principles of the methodology for calculating the phonon spectra and density of states show that the consistent use of the requirements of hyperspace symmetry, which is implemented in the application of sets of modulation vectors, features of the components of matrices A and B allows us to consistently form a procedure for calculating the dispersion dependences of phonons, and the choice of an array of force constant values allows us to achieve a satisfactory coincidence of the calculation results with the data of other authors.

REFERENCES

[1] P. M. De Wolff, T. Janssen, A. Janner, Acta Cryst. A37,. pp.625-636, 1981/

[2] A. Janner, T. Janssen, Phys. Rev. B 15, pp. 643 – 658, 1977.

[3] T. Janssen, J. Phys. C: Solid State Phys,. 12, 24. pp. 5381–5392, 1979

[4] I.I. Nebola, A.F. Katanytsia, A.Ya. Shteyfan, I.M. Shkyrta, I.P. Studenyak, M. Timko, P. Kopčanský, Semiconductor Physics, Quantum Electronics & Optoelectronics, vol. 23, No. 4. pp. 366–371, 2020.

[5]https://maple.cloud/app/5753562177994752/Modeling+of+dispersions+of+phonon+spectra.

[6] H.M. Tütüncü, H.Y. Uzunok, G.P. Srivastava, V. Özdemir, G. Uğur, Intermetallics, 96, pp 25-32, 2018

[7]https://www.sciencedirect.com/science/article/abs/pii/S0966979517311962#undfig

RESULTS

$$B = \rho_{ij}(q_i - q_j) = \begin{pmatrix} \rho_1 & \rho_2 & \rho_3 & \cdot & \cdot & \rho_{62} & \rho_{63} & \rho_{64} \\ \rho_2 & \rho_1 & \rho_1 & \cdot & \cdot & \rho_{61} & \rho_{62} & \rho_{63} \\ \rho_3 & \rho_2 & \rho_1 & \cdot & \cdot & \rho_{60} & \rho_{61} & \rho_{62} \\ \cdot^{\cdot} & : & \cdot_{\cdot} & \cdot & \cdot & \cdot_{\cdot} & : & \cdot^{\cdot} \\ \rho_{62} & \rho_{61} & \rho_{60} & \cdot & \cdot & \rho_1 & \rho_2 & \rho_3 \\ \rho_{63} & \rho_{62} & \rho_{61} & \cdot & \cdot & \rho_2 & \rho_1 & \rho_2 \\ \rho_{64} & \rho_{83} & \rho_{62} & \cdot & \cdot & \rho_3 & \rho_2 & \rho_1 \end{pmatrix} \otimes \begin{pmatrix} 1 & 0 & 0 \\ 0 & 1 & 0 \\ 0 & 0 & 1 \end{pmatrix}$$

$$\mathrm{A} = \rho\left(D^{\mathcal{P}}_{\beta\gamma}(k+q_i),(q_i-q_j)\right) = \rho\left(D_{(q_i-q_j)}(k+q_j)\right) = D_{(q_i-q_j)}(k,q_j) =$$

$$= \begin{pmatrix} D_{q_1}(k,q_1) & D_{q_2}(k,q_1) & D_{q_3}(k,q_1) & \cdot & \cdot & \cdot & D_{q_{62}}(k,q_1) & D_{q_{63}}(k,q_1) & D_{q_{64}}(k,q_1) \\ D_{q_2}(k,q_2) & D_{q_1}(k,q_2) & D_{q_3}(k,q_2) & \cdot & \cdot & \cdot & D_{q_{61}}(k,q_2) & D_{q_{62}}(k,q_2) & D_{q_{63}}(k,q_2) \\ D_{q_3}(k,q_3) & D_{q_{31}}(k,q_3) & D_{q_1}(k,q_3) & \cdot & \cdot & \cdot & D_{q_{60}}(k,q_3) & D_{q_{61}}(k,q_3) & D_{q_{61}}(k,q_3) \\ & \cdot\ \cdot\ \cdot & & \cdot & \cdot & \cdot & & \cdot\ \cdot\ \cdot & \\ & \cdot\ \cdot\ \cdot & & \cdot & \cdot & \cdot & & \cdot\ \cdot\ \cdot & \\ & \cdot\ \cdot\ \cdot & & \cdot & \cdot & \cdot & & \cdot\ \cdot\ \cdot & \\ D_{q_{62}}(k,q_{62}) & D_{q_{61}}(k,q_{62}) & D_{q_{60}}(k,q_{62}) & \cdot & \cdot & \cdot & D_{q_1}(k,q_{62}) & D_{q_2}(k,q_{62}) & D_{q_3}(k,q_{62}) \\ D_{q_{63}}(k,q_{63}) & D_{q_{62}}(k,q_{63}) & D_{q_{61}}(k,q_{63}) & \cdot & \cdot & \cdot & D_{q_2}(k,q_{63}) & D_{q_1}(k,q_{63}) & D_{q_2}(k,q_{63}) \\ D_{q_{64}}(k,q_{64}) & D_{q_{63}}(k,q_{64}) & D_{q_{62}}(k,q_{64}) & \cdot & \cdot & \cdot & D_{q_3}(k,q_{64}) & D_{q_2}(k,q_{64}) & D_{q_1}(k,q_{64}) \end{pmatrix}$$

Interacting atoms	Distance between atoms	Tensor values of the force constants in n/m
A, A	2a	[40.0, 30.0, 30.0], [30.0, 40.0, 30.0], [30.0, 30.0, 40.0]
A, B	$\sqrt{5}a$	[35.0, 30.0, 30.0], [30.0, 35.0, 30.0], [30.0, 30.0, 35.0]
A, A	$\sqrt{6}a$	[20.0, 10.0, 10.0], [10.0, 20.0, 10.0], [10.0, 10.0, 20.0]
B, B	$\sqrt{12}a$	[14.50, 11.0, 11.0], [11.0, 14.50, 11.0], [11.0, 11.0, 14.50]
A, B	$\sqrt{13}$a	[2.0, 1.0, 1.0], [1.0, 2.0, 1.0], [1.0, 1.0, 2.0]
A, A	$\sqrt{14}$a	[1.0, .5, .5], [.5, 1.0, .5], [.5, .5, 1.0]
B, B A, A	4a	[1.53, .7, .7], [.7, 1.53, .7], [.7, .7, 1.53], [1.5, .8, .8], [.8, 1.5, .8], [.8, .8, 1.50]

Table 1

Mode Frequencies at the R Point (THz)	Phonon Spectrum	Density of States
6.158229273640114, 6.158229274441641, 6.158229274583447, 6.158229274769974, 6.318938506392378, 6.318938507246698, 6.318938507516334, 6.318938507652525, 6.318938507854659, 6.318938508637496, 7.028092766031219, 7.028092766758334, 7.028092767157368, 7.028092767717506 5, 7.028092767719037, 7.028092768349351, 7.8745978840704085, 7.8745978842763575, 11.698130243417612, 11.69813024364457, 11.698130243765192, 11.698130245242007, 11.698130245436868, 11.698130246456614	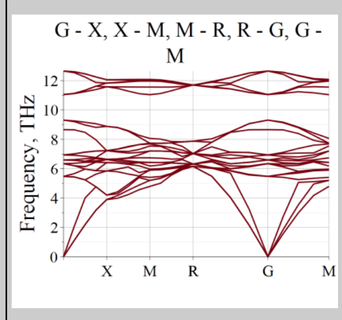 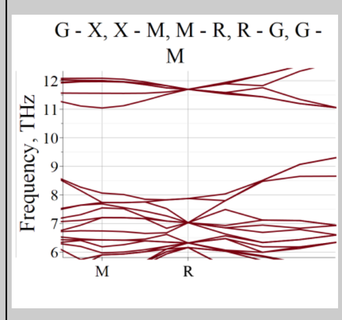	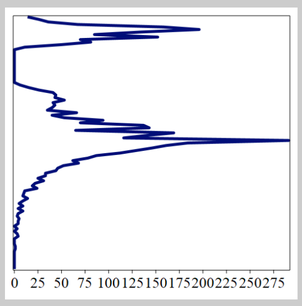

Table 2. V_6Si_2

Mode Frequencies at the R Point (THz)	Phonon Spectrum	Density of States
4.560132556188072 4 4.699858308078237 6 5.306372815117943 6 5.83109341681061 2 11.4224369276743 6	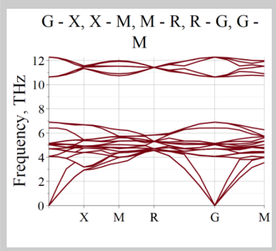 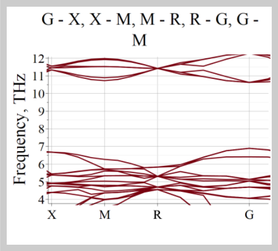	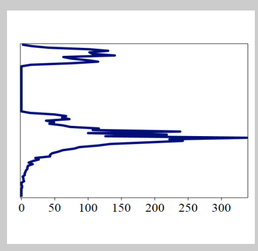

Table 3. Nb_6Si_2

Mode Frequencies at the R Point (THz)	Phonon Spectrum	Density of States
4.40122464244273 6 4.56013255553655 4 4.86942713916208 6 5.83109341702304 2 6.46464654212079 6	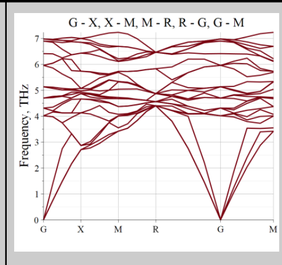 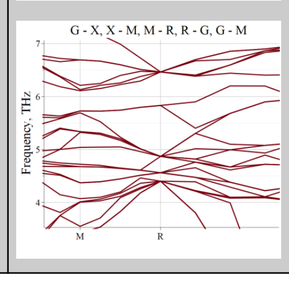	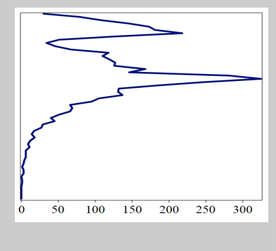

Table 4. Nb_6Sn_2